

DRAGON'S LAIR: ON THE LARGE-SCALE ENVIRONMENT OF BL LAC OBJECTS

F. MASSARO^{1,2,3,4}, A. CAPETTI², A. PAGGI^{1,2,3}, R. D. BALDI^{1,5},
A. TRAMACERE⁶, I. PILLITTERI⁷ & R. CAMPANA⁸

version January 2, 2022: fm

ABSTRACT

The most elusive and extreme sub-class of active galactic nuclei (AGNs), known as BL Lac objects, shows features that can only be explained as the result of relativistic effects occurring in jets pointing at a small angle with respect to the line of sight. A long standing issue is the identification of the BL Lac parent population, having jets oriented at larger angles. According to the “unification scenario” of AGNs, radio galaxies with low luminosity and edge-darkened radio morphology are the most promising candidates to be the parent population of BL Lacs. Here we compare the large-scale environment, an orientation independent property, of well-defined samples of BL Lacs with samples of radio-galaxies all lying in the local Universe. Our study reveals that BL Lacs and radio galaxies live in significantly different environments, challenging predictions of the unification scenario. We propose a solution to this problem proving that large-scale environments of BL Lacs is statistically consistent with that of compact radio-sources, known as FR0s, sharing similar properties. This implies that highly relativistic jets are ubiquitous and are the natural outcome of the accretion of gas into the deep gravitational potential well produced by supermassive black holes.

1. INTRODUCTION

Since the early 70's, extended radio galaxies were divided in two main types based on their radio morphology, distinguishing between edge-darkened (FRI type) and edge-brightened (FRII type) sources (Fanaroff & Riley 1974). For decades this dichotomy, was linked to their radio power and their large-scale environments having FRI is that generally inhabit galaxy-rich environments, being members of groups or galaxy clusters, while FRIIs live more isolated (Zirbel et al. 1997, see e.g.,). Radio galaxies were also classified on the basis of their optical spectra (Hine & Longair 1979), distinguishing between high and low excitation radio galaxies (HERGs and LERGs, respectively). While LERGs can show both FRI or FRII radio morphology (see e.g., Laing et al. 1994) HERGs appear to be, almost exclusively, FRIIs (see also Heckman et al. 2014).

Furthermore, it is becoming clear that the majority of low redshift radio galaxies are compact sources. These, known as FR0s, have with typical sizes $\lesssim 10kpc$ and are characterized by a LERG spectrum (Bladi et al. 2015) and as recently showed tend to live in poorer environments with respect to extended radio sources (Capetti et al. 2020).

On the other hand, BL Lac objects (hereinafter BZBs) are now recognized as the most extreme class of AGNs. Emitting from radio to TeV energies, they constitute the largest population of gamma-ray sources (Abdollahi et al. 2020) and show several peculiar observational properties including: flat radio spectra (Healey et al. 2007; Massaro et al. 2013), apparent superluminal motions (Lister et al. 2013), extreme variability up to TeV energies (Aharonian et al. 2007), high radio-to-optical polarization (Pavlidou et al. 2014), peculiar mid-infrared colors (Massaro et al. 2011) and featureless optical spectra, with only weak emission/absorption features (Stickel et al. 1991). At the Pittsburgh Conference in 1978 Blandford and Rees proposed to interpret all these features as non-thermal emission arising from particles flowing in a relativistic jet observed at a small angle with respect to the line of sight.

According to the “unification scenario” of radio-loud AGNs, at zeroth order, all jetted AGNs are intrinsically the same but they appear diverse due to different orientations with respect to the line of sight (Urry & Padovani 1995). This idea immediately prompted the quest for the identification of misaligned BZBs. Among radio-loud AGNs, radio galaxies, mainly those belonging to the FRI radio class (Fanaroff & Riley 1974), having low luminosity and an edge-darkened radio morphology, were naturally identified as the BZB parent population, since they also produce relativistic jets, extending up to hundreds of kiloparsec scales and lack broad emission lines.

There is a vast literature of tests on the validity of this unification scenario, in particular, those performed on the basis of the study of the large-scale environments (see e.g., Villarroel et al. 2014; Zou et al. 2019), an orientation independent property of AGNs (Antonucci & Ulvestad 1985). Here we carry out a statistical environmental test of the “unification scenario”, comparing a selected sample of BZBs with both

¹ Dipartimento di Fisica, Università degli Studi di Torino, via Pietro Giuria 1, I-10125 Torino, Italy.

² INAF-Osservatorio Astrofisico di Torino, via Osservatorio 20, 10025 Pino Torinese, Italy.

³ Istituto Nazionale di Fisica Nucleare, Sezione di Torino, I-10125 Torino, Italy.

⁴ Consorzio Interuniversitario per la Fisica Spaziale, via Pietro Giuria 1, I-10125 Torino, Italy.

⁵ Department of Physics and Astronomy, University of Southampton, Highfield, SO17 1BJ, UK.

⁶ University of Geneva, Chemin d'Ecogia 16, Versoix, CH-1290, Switzerland.

⁷ INAF-Osservatorio Astronomico di Palermo G.S. Vaiana, Piazza del Parlamento 1, 90134, Italy.

⁸ INAF/OAS, via Piero Gobetti 101, I-40129, Bologna, Italy.

(i) FRIs and (ii) LERGs, aiming at verifying if radio galaxies and BZBs inhabit the same galaxy-rich large-scale environments.

We adopt cgs units for numerical results and we assume a flat cosmology with $H_0 = 69.6 \text{ km s}^{-1} \text{ Mpc}^{-1}$, $\Omega_M = 0.286$ and $\Omega_\Lambda = 0.714$ (Bennett et al. 2014), unless otherwise stated, as adopted in previous analyses (see Massaro et al. 2019; Massaro et al. 2020, hereinafter M19 and M20, respectively).

2. SAMPLE SELECTION

We combined sources listed in the FRICAT with those of the sFRICAT sample for a total of 209 FRIs (Capetti et al. 2017a). The former sample lists FRIs at redshifts $z_{\text{src}} \leq 0.15^9$, selected to have a radio structure extending beyond 30 kpc, measured from the location of the host galaxy as seen in the optical band, while the latter includes 14 FRIs with radio emission between 10 and 30 kpc and $z_{\text{src}} \leq 0.05$. Then we also considered 101 FRIIs, in the same redshift range and all classified as LERGs, collected out of the FRIICAT (Capetti et al. 2017b) to obtain a sample of 310 LERGs. Both FRICAT and FRIICAT are based on data available in the Sloan Digital Sky Survey (see e.g., Ahn et al. 2012) and the Faint Images of the Radio Sky at Twenty-cm survey (FIRST White et al. 1997).

In our analysis we also performed a comparison with 108 FR0 radio galaxies selected in Baldi et al. (2018). These are all radio galaxies with (i) $z_{\text{src}} < 0.05$ being (ii) optically classified as LERG, with (iii) a radio flux density at 1.4 GHz in the FIRST survey above 5 mJy and (iii) lacking extended radio emission beyond a few kpc.

For BZBs we selected only those lying in the same SDSS central footprint and having a firm redshift estimate at $z_{\text{src}} \leq 0.15$, all out of the 5th release of the Roma-BZCAT (Massaro et al. 2015) for a total of 11 sources. Then we also added 3 more BZBs lying at $z_{\text{src}} < 0.15$ that were recently discovered thanks to our optical spectroscopic follow up campaign of low energy counterparts for the unidentified γ -ray sources (Massaro et al. 2012a; Massaro et al. 2016; de Menezes et al. 2019; Peña-Herazo et al. 2020). Thus the final sample of BZBs considered in our analysis lists 14 in the same redshift bin of radio galaxies.

For a comparison with literature results we also considered BL Lacs-galaxy dominated (hereinafter BZGs) listed in the Roma-BZCAT. Adopting the same criteria as for the BZB selection we extracted 41 BZGs lying between $0.02 < z < 0.15$ and with 14 out of 41 being associated with a γ -ray source (Abdollahi et al. 2020). BZGs are radio sources whose multifrequency emission exhibits some properties of BL Lacs but appears dominated by the host galaxy contribution, in particular in the optical-ultraviolet energy range. It is not yet clear if BZGs are all genuine BZBs, in a quiescent state given the high variability that BL Lacs show, or are moderately bright AGNs whose non-thermal emission does not present evidence for relativistic beaming (see also Massaro et al. 2012b).

3. INVESTIGATING LARGE-SCALE ENVIRONMENTS

⁹ z_{src} indicates the source redshift while z_{cl} that of a possible nearby galaxy group/cluster.

The comparison between large-scale environments of BZB, FRI and LERG samples, all in the SDSS central footprint, is carried out adopting the same procedure of M19 and M20. We used the number of cosmological neighbors to estimate the environmental richness. These are defined as all optical sources with SDSS magnitude flags indicating a galaxy-type object and having a spectroscopic z with $\Delta z = |z_{\text{src}} - z| \leq 0.005$, thus corresponding to the maximum velocity dispersion in groups and clusters of galaxies (see Berlin et al. 2006, e.g.). We indicate their number as N_{cn}^{500} and N_{cn}^{2000} , for those lying within 500 kpc and 2 Mpc from the central source, respectively. In Table 1 all parameters estimated for each sample analyzed here. In Figure 1 we show the R band optical image of the field around one BZB and one FRI in our samples with all cosmological neighbors highlighted.

As previously carried out to compare large-scale environments of two different classes we performed the following statistical tests. The first is based on N_{cn}^{500} , i.e., medians of the N_{cn}^{500} distribution, while the second applying the Mann-Whitney U rank. To avoid cosmological effects both tests performed in each redshift bin of 0.01 size (see M20 for details).

We also compared the environment of FR0s with that of BZBs. However, since the FR0 sample is limited to $z = 0.05$, we simulate how galaxy over-density surrounding FR0s would be detected if they lie at larger redshift adopting the same strategy of Capetti et al. (2020). Thus assuming that large-scale environments of FR0s does not evolve in the redshift range between 0.05 and 0.15, we computed the absolute magnitude in the R band of all cosmological neighbors and, maintaining their intrinsic power, we rescaled it at larger distances, i.e. in all redshift bins where there is at least one BZB. We also recomputed accordingly radii of 500 kpc and 2 Mpc in each redshift bin. We measured the number of cosmological neighbors with rescaled apparent magnitude m_r brighter than 17.8 corresponding to the SDSS criterion to select spectroscopic targets. These simulations allow us to measure expected medians of cosmological neighbors within 500 kpc and 2 Mpc circles for FR0s up to $z = 0.15$.

These simulations were tested over the FRI samples. Under the same assumptions previously described, we computed median values of all cosmological neighbors surrounding simulated FRIs in all redshift bins up to $z = 0.15$ where there is at least one BZB and we found a perfect agreement with the observed values being 4 at $z = 0.065$, 3 at $z = 0.075$ and 1 at $z = 0.105$, 0.125 and 0.135, as reported in the following.

4. RESULTS

The median values $\bar{N}_{\text{cn}}^{500}$ for both samples of FRIs and LERGs are shown in Fig. 2. It is clear that the measured values of N_{cn}^{500} for all 14 BZBs lying at $z_{\text{src}} \leq 0.15$ lie all systematically below the $\bar{N}_{\text{cn}}^{500}$ of both radio galaxy sample. Then comparing $\bar{N}_{\text{cn}}^{2000}$ the situation is in agreement with previous results with only 3 out of 14 BZBs for which $\bar{N}_{\text{cn}}^{2000}$ is marginally consistent with that of radio galaxies (i.e., FRIs and LERGs).

In Fig. 2 we show, above each N_{cn} median value of the two RG distributions of the normalized z_U variable computed for the Mann-Whitney U test when comparing

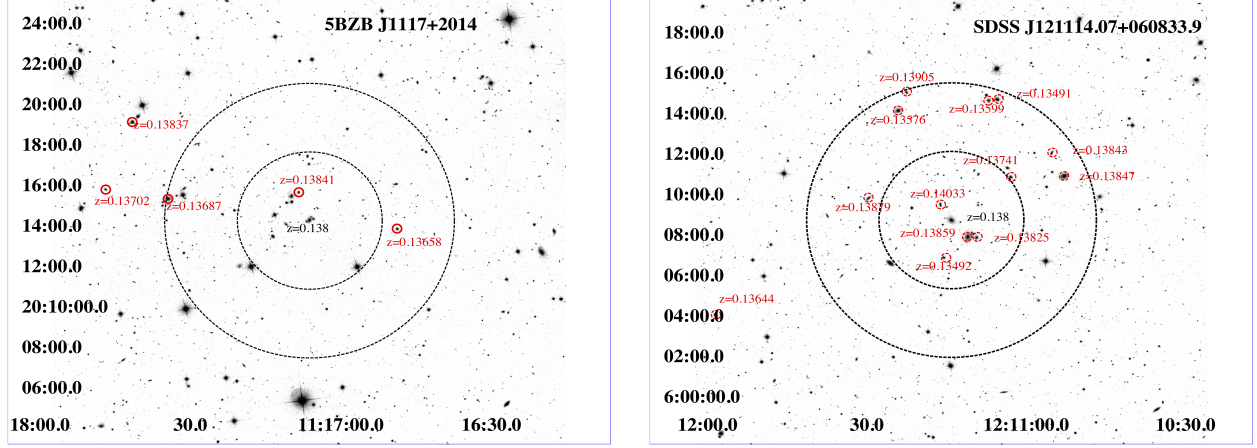


Figure 1. *Left)* The R -band SDSS image of the field surrounding 5BZB J1117+2014 centered on its position. Two lack circles have radius of 500kpc and 1Mpc, respectively, computed at the central source redshift. All cosmological neighbors are marked with a red circle and have their $z_{\text{src}} < \text{reported}$. In our sample 5BZB J1117+2014 has the largest number of cosmological neighborhoods within 2 Mpc. *Right)* Same as left panel for the FR I SDSS J121114.07+0608339 at the same redshift of 5BZB J1117+2014, both reported close to their positions in black. It is quite evident as SDSS J121114.07+0608339 has a large-scale environment richer of galaxies than 5BZB J1117+2014. In both figures cosmological neighbors are brighter than 17.8 magnitudes in the R band (i.e.. the SDSS threshold to select spectroscopic targets).

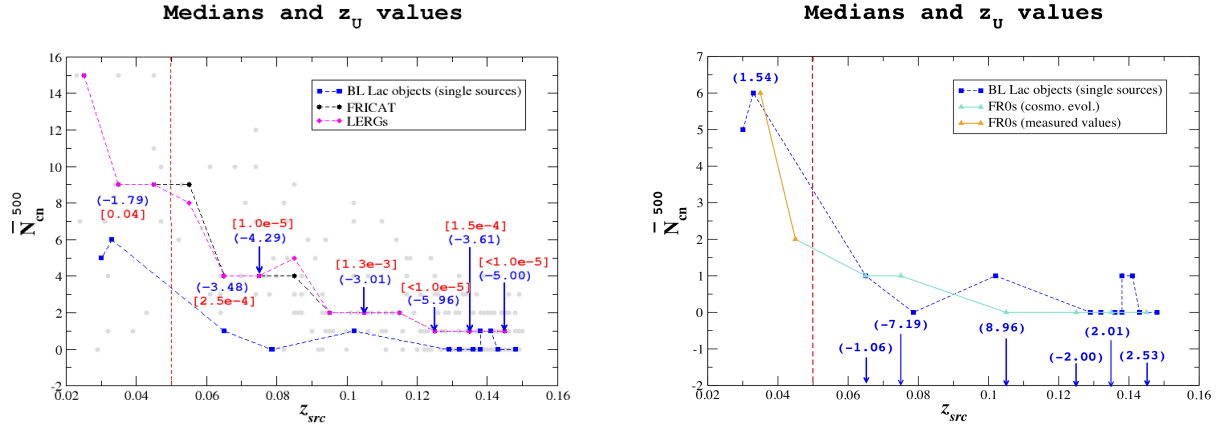


Figure 2. *Left)* Medians of N_{cn}^{500} for FRIs (black circles) and LERGs (magenta diamonds) per redshift bins of 0.01 size. Blue squares corresponds to the values for single BZBs at $z_{\text{src}} < 0.15$ Blue numbers reported in parenthesis close to each median of LERGs correspond to values computed for the z_U normalized variable of the Mann-Whitney U rank test performed between BZBs and LERGs (see §. 3 for details) while red numbers correspond to the p-values. As shown BZBs are distributed systematically below all medians of both FRIs and LERGs thus indicating that they inhabit less galaxy-rich large-scale environments. All grey circles shown in the background correspond to the single values of N_{cn}^{500} for all considered LERGs. *Right)* Same as left panel but reporting the comparison between BZBs and FR0s. Orange triangles are measured medians below $z_{\text{src}} = 0.05$ while cyan triangles refer to simulated medians between $0.05 < z < 0.15$ for each bin where there is at least one BZB. It is remarkable the agreement between both measured and estimated/simulated medians of the FR0 population and that of BZBs, indicating that the former could be the parent population of BZBs. Vales of the normalized z_U variable are also reported.

BZBs with LERGs. This is again systematically negative and not consistent with zero within more than a 3σ level of confidence, with the only exception of a single bin between $z = 0.03$ and $z = 0.04$. The latter statistical tests were performed in each redshift bin thus grouping BZBs as LERGs.

Both statistical tests allows us to claim that the hypothesis that large-scale environments of BZBs and that of FRIs and/or LERGs are similar can be rejected with high level of confidence, with a chance probability of 10^{-4} for the median test. This implies that FRIs or more in general LERGs inhabit richer large-scale environments than BZBs and cannot be their “parent” population as

predicted by the AGN unification scenario.

Finally, we compared large-scale environments of BZBs and FR0s where measured values of N_{cn}^{500} and N_{cn}^{2000} of FR0s are only available at $z_{\text{src}} < 0.05$. However, adopting simulations previously described (see § 3) we “extrapolated” the behavior of FR0 environments up to $z = 0.15$. As shown in Fig. 2 values of N_{cn}^{500} for BZBs and FR0s, both measured (i.e., below $z = 0.05$) and extrapolated up to $z = 0.15$ with the median test and or using the z_U normalized variable appear indistinguishable.

5. COMPARISON WITH THE LITERATURE

The largest fraction of all analyses carried out to date on BZB large-scale environments are mainly focused on single sources and small samples (see e.g., Arp 1970; Disney 1974; Craine et al. 1975; Stickel et al. 1991; Torres-Zafra et al. 2018; Rovero et al. 2016), with several being based on photometric companion galaxies in their neighborhoods (Falomo et al. 1990; Falomo et al. 1993a; Falomo et al. 1993b; Wurtz et al. 1993; Pesce et al. 1994; Pesce et al. 1995; Falomo et al. 1995; Muriel et al. 2015). However results appear to be still controversial and contradictory.

Then in 2016 the comparison between BZBs listed in the Roma-BZCAT and sources belonging to the catalog of galaxy clusters and groups of Merchà & Zandivarez (2005) was presented (Muriel 2016). This is the first statistical analysis over a large sample of BL Lacs. Muriel (2016) found that 121 blazars appear to be associated with sources listed in the cluster catalog, these are classified as: 24 BZBs, 96 BZGs and 1 BZUs according to the Roma-BZCAT. Restricting the analysis to redshifts below ~ 0.2 , where the cluster catalog is less incomplete the number of spatial coincidences decreases to 78. Taking into account the contamination by spurious groups/clusters of galaxies only $43 \pm 5\%$ of all BL Lac objects, including BZGs, lie in groups of three or more members, where the expected fraction computed for a random sample of galaxies, having the same redshift distribution, is $19.3 \pm 0.1\%$. Muriel et al. (2016) also applied a correction factor due to the redshift incompleteness of the algorithm used to create the galaxy cluster/group catalog then claiming a BZB fraction in groups of $\sim 67 \pm 8\%$ for all 78 sources.

According to the Roma-BZCAT, BZGs are not “genuine” blazars, but could be moderately bright AGNs whose non-thermal emission does not present evidences for relativistic beaming and/or are misclassified sources. Thus we analyzed BZGs analyzed separately from BZBs. In Figure 3 we compared BZBs and BZGs and found that values of cosmological neighbors for BZGs are consistent with those of radio galaxies. Thus mixing BZBs with BZGs, given the larger number of BZGs at $z < 0.15$ (i.e., 129 in the Muriel sample) they could bias the whole statistical analysis. Moreover, Muriel (2016) that also did not consider any constraint on the “redshift distance” between BZBs and nearby galaxy clusters thus neglecting spurious association.

To further explore the BZB *vs* BZG “dichotomy” we assumed that all BZGs associated with a γ -ray source are “real” BZBs having dimmed jet emission below the host galaxy component. Then we doubled the BZB sample and we run again our comparative analysis between them and the LERGs. We found no differences with respect to the previous results with the only exception of one redshift bin between centered at 0.075 where there are only two BZGs, namely 5BZG J0809+3455 and 5BZG J0829+1754. However we inspected their FIRST radio maps and they show clear extended radio structures (i.e., lobes and plumes) beyond tens of kpc thus being very different from BZBs and being classical LERGs.

An analysis based on similar samples used here, comparing FRIs and BZBs, has been recently carried out (see Sandrinelli et al. 2019, for details) using the average excess of galaxy surface density E_r . As extensively discussed in Massaro et al (2019, 2020) this method has sev-

eral statistical and cosmological uncertainties. An analysis performed without removing these biases will show that the higher redshift population tend to inhabit less galaxy-rich large-scale environments.

Moreover this method improperly average measurements of E_r with different signal-to-noise ratios (SNRs) and compare sources in different redshift bins thus including cosmological artifacts. To illustrate this SNR effect in Fig. 4 we show SDSS sources around two FRIs, namely SDSS J132017.54+043037.4 at $z_{\text{src}} = 0.146$ and SDSS J135302.04+330528.5 at $z_{\text{src}} = 0.061$ together with all background and foreground galaxies within a circular region of 500 kpc. Surrounding galaxies N_{sel} are selected to have SDSS flags $q_{\text{mode}}=1$, $Q>2$, $cl=3$ and $ic=3$ and an absolute magnitude in the i band, computed at the same distance of the central source, greater than -21 . The number of background galaxies n_{bg} , reported with its standard deviation in parenthesis, was estimated adopting the same criteria previously mentioned and averaging on 20 regions of the same area centered, at angular separation greater than 4 Mpc from the central source. Both measurements clearly show an excess of galaxies is marginally significant ($\sim 1\sigma$), thus being consistent with a background fluctuations and averaging over these measurements does not appear statistically correct. This makes challenging any comparison with our results.

6. SUMMARY AND CONCLUSIONS

In the present analysis we focused on the comparison between large-scale environments of BZBs and radio galaxies at similar redshifts. This is the key to obtain robust results that guarantee to avoid statistical biases and cosmological artifacts affecting most of previous analyses (see § 5 for comparison with the literature). Our analysis is carried out counting the number of cosmological neighbors, i.e., optical galaxies with a firm spectroscopic redshift and with velocities within the maximum velocity dispersion of sources belonging to galaxy groups and clusters.

Results achieved can be summarized as follows.

1. In the local Universe the large-scale environment of BZBs is systematically different from that of both FRIs and LERGs suggesting that the unification scenario of radio-loud AGNs must be revised.
2. However, a direct comparison between environmental properties of BZBs and the low power “compact” radio galaxies, known as FR0s, reveals that their large-scale environments are indistinguishable. This suggests that FR0s could be the parent population of BZBs.
3. Comparing BZBs and BZGs we also found that the latter class appears to have large-scale environments more similar to LERGs thus unlikely to be all “weak” BZBs.
4. Investigations of large scale environments based on the average excess of galaxy surface density does not appear statistically robust being affected by cosmological artifacts and uncertainties due to the SNR.

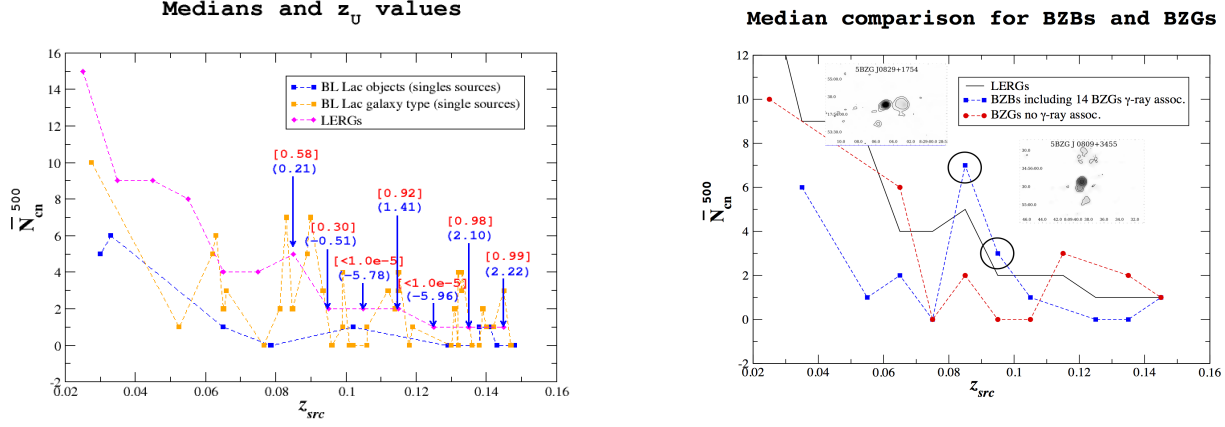


Figure 3. Left) Same of Fig. 2 but comparing BZBs and BZGs. Here it is quite evident the agreement between BZGs and LERGs with the former class being more separated from BZBs. Right) The comparison between the BZB medians, including all BZGs associated to γ -ray sources being considered as weak BZBs, and all remaining BZGs. Two black circles highlight z bins where there are mostly BZGs and that at $z = 0.075$ where the two BZGs show extended radio structures highlighted with radio contour maps at 1.4 GHz drawn at levels of 0.0005, 0.0025, 0.125, 0.625 Jy.

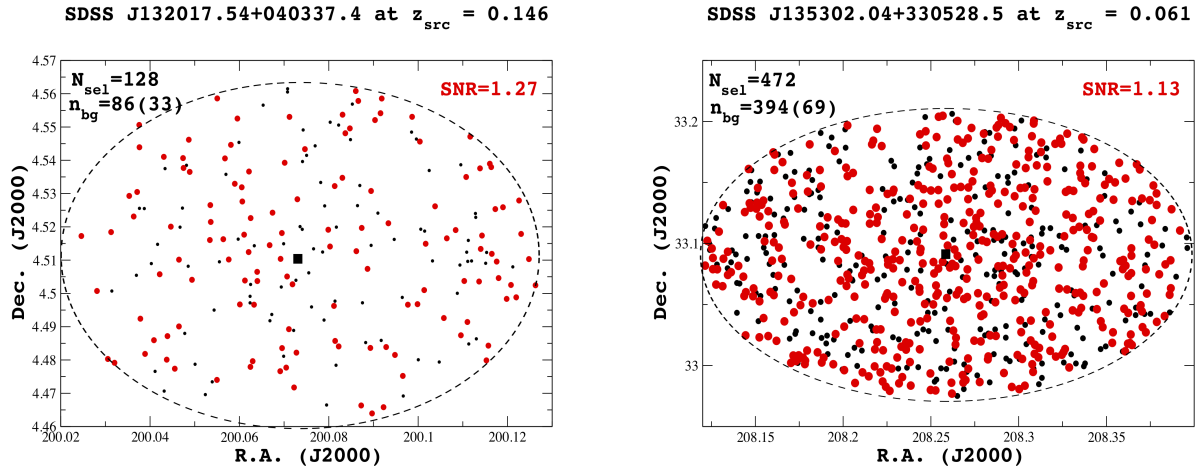


Figure 4. All SDSS sources lying within 500 kpc (black ellipse), computed at the redshift of two FR Is, lying in the center of both images: SDSS J132017.54+040337.4 (left) and SDSS J135302.04+330528.5 (right). Black circles mark sources listed as galaxies according to SDSS flags (see § 5 for details) while those brighter than absolute magnitude in the i band equal to -21, computed at the redshift of the central radio galaxy are red and their number is N_{sel} . The number of background galaxies n_{bg} is also reported, with its standard deviation in parenthesis in both images together with the signal to noise ratio (SNR), computed averaging the galaxy count, adopting the same i band magnitude selection, over 20 regions of the same area centered at angular separation greater than 4 Mpc, from the central sources, and is reported in Fig. 4. Both measurements clearly show as excess of the galaxy number density $E_r = N_{sel} - n_{bg}$ is consistent with a background fluctuations at less than 2σ (i.e., as an upper limit).

We conclude that BZBs are mainly aligned counterparts of compact FR0s and only in extreme cases LERGs. This correspondence between BZBs and FR0s, both hosted in massive elliptical galaxies, points towards the ubiquitous presence of relativistic jets as natural outcome of gas accretion into the deep gravitational potential well produced by supermassive black holes.

F. M. wishes to thank Dr. C. C. Cheung for their valuable discussions on this project planned during the organization of the IAU 313 Symposium. This work is supported by the “Departments of Excellence 2018 -

2022” Grant awarded by the Italian Ministry of Education, University and Research (MIUR) (L. 232/2016). This research made use of resources provided by the Ministry of Education, Universities and Research for the grant MASF_FABR_17.01. This investigation is supported by the National Aeronautics and Space Administration (NASA) grants GO9-20083X. TOPCAT and STILTS astronomical software (Taylor 2005) were used for the preparation and manipulation of the tabular data and the images.

REFERENCES

Table 1
Environmental parameters for all sample analyzed (first 10 lines).

Sample	Name	R.A. (J2000) hh:mm:ss.ss	Dec. (J2000) hh:mm:ss.ss	z_{src}	Δz	d_{proj} (kpc)	N_{cn}^{500}	N_{cn}^{1000}	N_{cn}^{2000}
FR0	SDSSJ010852.48-003919.4	01:08:52.48	-00:39:19.40	0.045	0.0012	303.05	2.0	6.0	7.0
FR0	SDSSJ011204.61-001442.4	01:12:04.61	-00:14:42.40	0.044	4.0E-4	556.58	0.0	1.0	1.0
FR0	SDSSJ011515.78+001248.4	01:15:15.78	+00:12:48.40	0.045	2.0E-4	173.27	27.0	39.0	39.0
FR0	SDSSJ015127.10-083019.3	01:51:27.10	-08:30:19.30	0.018	2.0E-4	30.75	12.0	13.0	13.0
FR0	SDSSJ020835.81-083754.8	02:08:35.81	-08:37:54.80	0.034	3.0E-4	413.79	1.0	2.0	2.0
LERG	SDSSJ073014.37+393200.4	07:30:14.37	+39:32:00.40	0.142	0.0011	207.56	1.0	4.0	6.0
LERG	SDSSJ073505.25+415827.5	07:35:05.25	+41:58:27.50	0.087	6.0E-4	758.0	3.0	4.0	10.0
LERG	SDSSJ073719.18+292932.0	07:37:19.18	+29:29:32.00	0.111	0.0034	826.91	1.0	1.0	5.0
LERG	SDSSJ074125.85+480914.3	07:41:25.85	+48:09:14.30	0.12	0.005	1890.54	0.0	0.0	1.0
LERG	SDSSJ074351.25+282128.0	07:43:51.25	+28:21:28.00	0.106	3.0E-4	258.8	4.0	4.0	9.0

Col. (1): Sample.
Col. (2): Source name.
Col. (3): Right Ascension.
Col. (4): Declination.
Col. (5): redshift.
Col. (6): Difference between the average redshift of cosmological neighbors in 2 Mpc and that of the central source.
Col. (7): Physical distance between the central RG and the average position of cosmological neighbors within 2 Mpc, computed at z_{src} .
Col. (8,9,10): Number of cosmological neighbors within 500, 1000 ad 2000 kpc, respectively.

Abdollahi, S.; Acero, F.; Ackermann, M.; Ajello, M.; Atwood, W. B. et al. 2020 ApJS, 247, 33
Aharonian F. et al., 2007 ApJ, 664, L71
Ahn, C. P., Alexandroff, R., Allende Prieto, C., Anderson, Scott F., Anderton, T. et al. 2012 ApJS, 203, 21
Antonucci, R. R. J.; Ulvestad, J. S. 1985 ApJ, 294, 158
Arp, H. 1970 ApL, 5, 75
Baldi, Ranieri D.; Capetti, Alessandro; Giovannini, Gabriele 2015 A&A, 576A, 38
Baldi, R. D.; Capetti, A.; Massaro, F. 2018 A&A, 609A, 1
Bennett, C. L., Larson, D., Weiland, J. L., Hinshaw, G. 2014 ApJ 794, 135
Berlind, A. A. et al. 2006 ApJS, 167, 1
Blandford, R. D., Rees, M. J., 1978, PROC. Pittsburgh Conference on BL Lac objects”, 328
Capetti, A., Massaro, F., Baldi, R. D. 2017 A&A 598A, 49
Capetti, A., Massaro, F., Baldi, R. D. 2017 A&A 601A, 81
Capetti, A.; Massaro, F.; Baldi, R. D. 2020 A&A, 633A, 161
Craine, E. R.; Tapia, S.; Tarengi, M. 1975 Natur, 258, 56
de Menezes, R., Peña-Herazo, H. A., Marchesini, E. J., et al. 2019, A&A, 630, A55
Disney, M. J. 1974 ApJ, 193L, 103
Falomo, Renato; Melnick, Jorge; Tanzi, Enrico G. 1990 Natur, 345, 692
Falomo, R.; Pesce, Joseph E.; Treves, A. 1993 AJ, 105, 2031
Falomo, R.; Pesce, Joseph E.; Treves, A. 1993 ApJ, 411L, 63
Falomo, Renato; Pesce, Joseph E.; Treves, Aldo 1995 ApJ, 438L, 9
Fanaroff, B. L., Riley, J. M. 1974 MNRAS 167, 31
Healey, Stephen E.; Romani, Roger W.; Taylor, Gregory B.; Sadler, Elaine M.; Ricci, Roberto et al. 2007 ApJS, 171, 61
Heckman, T. M. & Best, P. N. 2014 ARAA 52, 589
Hine, R. G.; Longair, M. S. 1979 MNRAS 188, 111
Laing, R. A.; Jenkins, C. R.; Wall, J. V.; Unger, S. W. 1994 The First Stromlo Symposium: The Physics of Active Galaxies. ASP Conference Series, Vol. 54, 1994, G.V. Bicknell, M.A. Dopita, and P.J. Quinn, Eds., p.201
Lister, M. L.; Aller, M. F.; Aller, H. D.; Homan, D. C.; Kellermann, K. I. et al. 2013 AJ, 146, 120
Massaro, E., Giommi, P., Leto, C. et al. 2009 A&A, 495, 691

Massaro, E., Giommi, P., Leto, C. et al. 2011 “Multifrequency Catalogue of Blazars (3rd Edition)”, ARACNE Editrice, Rome, Italy
Massaro, F.; D’Abrusco, R.; Tosti, G.; Ajello, M.; Paggi, A.; Gasparrini, D. 2012 ApJ, 752, 61
Massaro, E., Nesci, R., Piranomonte, S. 2012 MNRAS 422, 2322
Massaro, F.; Giroletti, M.; Paggi, A.; D’Abrusco, R.; Tosti, G.; Funk, S. 2013 ApJS, 208, 15
Massaro, E., Maselli, A., Leto, C. et al. 2015 Ap&SS, 357, 75
Massaro, F.; Álvarez Crespo, N.; D’Abrusco, R.; Landoni, M.; Masetti, N. et al. 2016 Ap&SS, 361, 337
Massaro, F.; Álvarez-Crespo, N.; Capetti, A.; Baldi, R. D.; Pillitteri, I. et al. 2019 ApJS, 240, 20
Massaro, F.; Capetti, A.; Paggi, A.; Baldi, R. D.; Tramacere, A. et al. 2020 ApJS in press
Merchán, Manuel E.; Zandivarez, Ariel 2005 ApJ, 630, 759
Muriel, H.; Donzelli, C.; Rovero, A. C.; Pichel, A. 2015 A&A, 574A, 101
Muriel, H. 2016 A&A, 591L, 4
Pavlidou, V.; Angelakis, E.; Myserlis, I.; Blinov, D.; King, O. G. et al. 2014 MNRAS, 442, 1693
Peña-Herazo, H. A. et al. 2020, A&A subm.
Pesce, J. E.; Falomo, R.; Treves, A. 1994 AJ, 107, 494
Pesce, Joseph E.; Falomo, Renato; Treves, Aldo 1995 AJ, 110, 1554
Rovero, A. C.; Muriel, H.; Donzelli, C.; Pichel, A. 2016 A&A, 589A, 92
Sandrinelli, A.; Falomo, R.; Treves, A. 2019 MNRAS, 485L, 89
Stickel, M.; Padovani, P.; Urry, C. M.; Fried, J. W.; Kuehr, H. 1991 ApJ, 374, 431
Taylor M. B., 2005, ASPC, 347, 29
Torres-Zafra, Juanita; Cellone, Sergio A.; Buzzoni, Alberto; Andruchow, Ileana; Portilla, José G. 2018 MNRAS 474, 3162
Urry, C. M., & Padovani, P. 1995, PASP, 107, 803
Villarreal, Beatriz; Korn, Andreas J. 2014 NatPh, 10, 417
White, R. L., Becker, R. H., Helfand, D. J.; Gregg, M. D. 1997 ApJ 475, 479
Wurtz, Ronald; Ellingson, Erica; Stocke, John T.; Yee, H. K. C. 1993 AJ, 106, 869
Zirbel, Esther L. 1997 ApJ, 476, 489
Zou, Fan; Yang, Guang; Brandt, William N.; Xue, Yongquan 2019 ApJ, 878, 11